
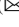





Normal Equilibrium Fluctuations from Chaotic Trajectories: Coupled Logistic Maps

Kyle Taljan¹  and J. S. Olafsen²  

¹ Case Western Reserve University, Yost Hall 2049 Martin Luther King Jr. Drive,
OH 44106-7058 Cleveland, USA

² Department of Physics, Baylor University, TX 76798 Waco, USA
Jeffrey_Olafsen@baylor.edu

Abstract. We report results of a numerical algorithm to examine coupling of two logistic maps where the mixing is chosen to maintain the stability of one map at the loss of the other. The long-term behavior of the coupling is found to contain windows in which the mixing results in Gaussian fluctuations about a fixed point for the stabilized map. This deterministic behavior is the result of the destabilized map simultaneously being driven into a chaotic regime and not noise. The results are applicable to both chaotic encryption of data and recapturing equilibrium behavior in a non-equilibrium system.

Keywords: Encryption · Nonlinear dynamics · Logistic maps

1 Introduction

Chaotic maps can be thought of as simple systems that demonstrate non-equilibrium behavior: deterministic systems that nonetheless take an essentially infinite amount of time to repeat themselves. Chaotic behavior can thus be classified as a certain type of steady-state dynamics that is the result of a small number of inputs. This picture is particularly beneficial in using the logistic map

$$Z_n + 1 = \mu z_n(1 - z_n) \quad (1)$$

as a simple system that at low values of the parameter μ demonstrates equilibrium behavior in the long-term mapping to a single point and demonstrates a period doubling path to chaos as μ is increased [1]. Studying non-equilibrium systems contributes to a better physical description of their poorly understood thermostatics. While it has been demonstrated that a proper selection of coarse graining [2] or particular control of the type of non-equilibrium balance between energy injection and dissipation [3] can result in a recapturing of equilibrium-like behavior and Maxwell-Boltzmann statistical fluctuations, a fundamental picture of the laws of non-equilibrium thermodynamics remains elusive. Chaotic maps, which themselves may be thought of as a subset of non-equilibrium systems [4], can also potentially aid in the encryption of information

for security purposes [5]. A set of coupled chaotic maps demonstrating an underlying Gaussian dynamic would also be beneficial for use as a deterministic manner in which to hide information in a signal that appears random [6].

Motivated by recent observations of a granular dimer on a vertically shaken plate [7], a set of coupled logistic maps were proposed as a potentially simple model of a two-component system with both a stable and unstable dynamic. This choice is because a single particle on an oscillating plate demonstrates a period doubling path to chaotic behavior. The shaken dimer demonstrates a breaking of symmetry where one sphere of the dimer appears to remain nearly stable with the shaken plate while the other chatters with a phase coherence that may demonstrate chaotic instability [8]. To model this dynamic, we proposed a specific pair of coupled logistic maps:

$$x_{n+1} = \mu_x x_n (1 - x_n) + \varepsilon x_n y_n \quad (2)$$

$$y_{n+1} = \mu_y y_n (1 - y_n) - \varepsilon x_n y_n \quad (3)$$

where the $\pm \varepsilon x_n y_n$ term provides the mixing between the two maps, x and y , via the small positive parameter, ε . Since the two uncoupled maps are independent and exist in a regime of $[0,1]$, the positive mixing term effectively increases the value of μ_x in Eq. 2 and destabilizes the x map by driving it further along the period doubling path to chaos while at the same time effectively decreases μ_y in Eq. 3 and stabilizes the y map for small values of ε . This is an example of a “master-slave” system [9, 10].

While the results will demonstrate a more immediate application to the encryption of data, initially this mixing was developed as a potential model of the effective cross term responsible for the anisotropic behavior observed in a dimer on a vertically shaken plate [11]. Because of this motivation, the μ_y values studied here were limited to a range over which the logistic map demonstrates a single stable fixed point, and μ_x was allowed to vary over a wider range of values. However, because the logistic map is only properly defined on the range of $[0, 1]$, the mixing parameter ε was purposely kept small in this study and limited to values in the range of $[0, 0.075]$. In this regime, the x map is destabilized while the net effect on the y map is to maintain the stability in a window about the fixed point. These choices also avoided errors with the double-precision calculation of the trajectories [12].

For $\varepsilon = 0$, the two maps are uncoupled and the typical logistic map behavior is of course recovered for each of $x(\varepsilon = 0) = y(\varepsilon = 0) = z$ as shown in Fig. 1. The squares in the range of $2.8 \leq \mu \leq 3.05$ denote the values for μ_y used in this study and the blue region centered about $\mu \sim 3.8$ the values of interest for μ_x that will be discussed later along with specific values of μ_x and μ_y indicated by the arrows. For comparison, when the mixing is turned on by allowing $\varepsilon > 0$, the behavior is quite different as demonstrated in Fig. 2(a) and (b) for the long-term trajectories of x and y , respectively, as a function of μ_x . (For the rest of this letter, the prescription was to select a value of μ_y that kept y at or near a stable fixed point, as shown as boxes in Fig. 1 for the uncoupled logistic map, and then to examine the coupled equations as a function of the parameter μ_x .) In Fig. 2, the value of μ_y is 2.95 and ε is 0.05. Careful examination of Fig. 2(a) for the coupled x map compared to the uncoupled z map of Fig. 1 confirms the general behavior

of ε for the x map is to effectively *increase* the value of μ_X . Note that the bifurcation to period 2 behavior that occurs in the uncoupled map for $\mu = 3.0$ in Fig. 1 occurs for the coupled x map in Fig. 2(a) at a slightly lower value of $\mu_X \sim 2.975$. In nearly every regard, the bifurcation diagram of x is simply the same as the uncoupled logistic map shifted slightly lower in μ_X (made more unstable) by the addition of the mixing term. (As an additional guide to the eye, the vertical arrow to the right side of Fig. 1 is at the same μ value as the vertical arrow in Fig. 2(a).) In Fig. 2(a) and 2(b), the long-term behavior of each trajectory at each μ_X is demonstrated by iterating the maps for 30,000 steps and plotting the last 20,000 iterations of each trajectory.

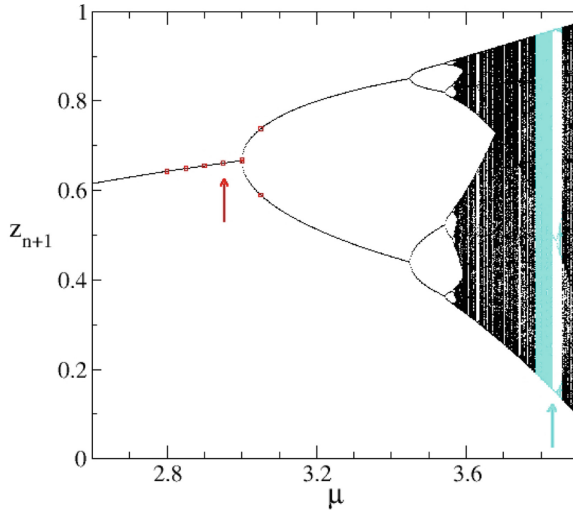


Fig. 1. The long-term behavior of the logistic map as a function of the parameter μ . The boxes on the left denote the μ_Y values used for the coupled y -map, while the shaded region on the right denotes the parameter space of interest for μ_X of the coupled x -map.

Far more interesting is the effect the mixing term has on the behavior of the y map. Even though μ_Y for the y map is held fixed at 2.95, and the lowest order effect of the $-\varepsilon x_n y_n$ term is to maintain that stability by effectively *reducing* μ_Y , the coupling adds fluctuations (from the x map) about what would be a stable fixed point without the coupling. In the periodic regions, these fluctuations simply behave as a self-similar version of the logistic map superimposed upon the stable fixed point of the uncoupled y map for $\mu_Y = 2.95$. One will also note that while the value of the fixed point moves for μ values in the range between 2.6 and 2.9 in Figs. 1 and 2 (a), the fixed point in the y map is stationary in Fig. 2(b). Yet, in the chaotic regions of the x map, the mixing term produces fluctuations that are different from the uncoupled logistic map in that they remain in a small window (of approximate size ± 0.05) about the stable fixed point for the uncoupled y map. The width of this window is determined by the value of ε .

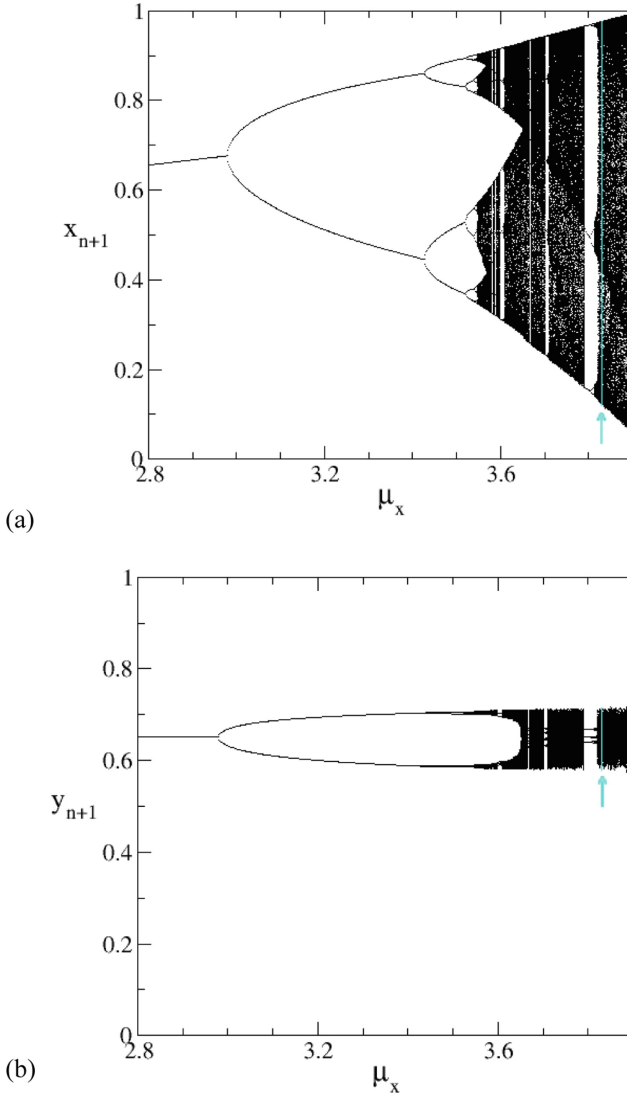


Fig. 2. The long-term behavior for the coupled maps (a) x_n and (b) y_n as a function of μ_X with $\mu_Y = 2.95$ and $\epsilon = 0.050$. The arrows denote the value of μ_X of interest discussed in Figs. 3 and 4.

2 Discussion

To characterize the fluctuations of the coupled y map about the fixed point from its uncoupled counterpart, one can examine the flatness of the distribution. The flatness of a set of values, v , is defined as the ratio of the fourth moment of the fluctuations from the mean of v to the square of the variance, or second moment, of the fluctuations of v :

$$F = \langle v^4 \rangle / \langle v^2 \rangle^2 \tag{4}$$

where a flatness $F = 3$ is the result for a Gaussian (normal) distribution [13]. Figure 3 is a plot of the flatness as determined by the second and fourth moments of the last 20,000 iterations of the long-term behavior of the coupled maps. (Note: The value of $F - 3$, demonstrating the deviation from Gaussian or the kurtosis, is what is plotted.) The lighter (blue) line is the result for the coupled x map, which is simply a shifted version of the uncoupled logistic map, while the darker (black) line is the result for the coupled y map. For both the x and y maps, in regions where the maps are single valued, the fourth and second moments are equal, resulting in a flatness of unity, so $F - 3 = -2$. The relative behavior of the flatness for the x and y maps in the range of $3.4 < \mu_X < 3.7$ also underscores that the y map is more stable than the x map by introduction of the mixing term.

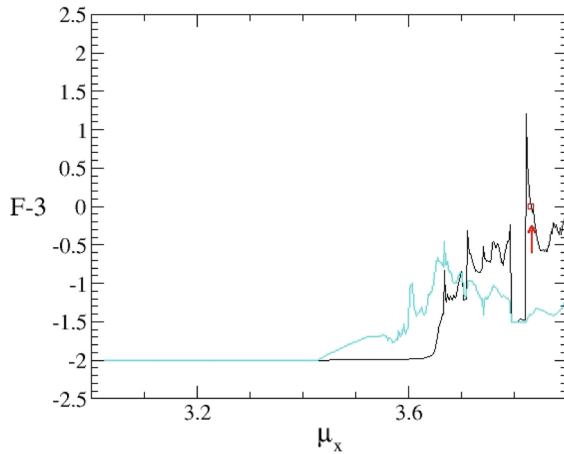


Fig. 3. The flatness of the distribution of x_n (blue) and y_n (black) points from the long-term behavior of the maps. The box and arrow denotes a situation where the y_n points form a Gaussian distribution.

Yet, in the regime of μ_X where the coupled y map exhibits period doubling, the flatness of the y map is generally closer to Gaussian than that for either the coupled x map or the uncoupled logistic map (not shown). Indeed, at just above $\mu_X = 3.8$, the plot of $F - 3$ of the fluctuations about the mean value for the y map rises above zero, before passing back through zero and becoming negative. The point where this occurs is denoted by the box and arrow in Fig. 3 as well as the vertical arrow in Fig. 2(b). This is a dynamic result of the mixing that occurs for a particular value of the parameters and is not due to additive noise [14] or computational imprecision [12].

At $\mu_X = 3.832$, the flatness of the fluctuations for the y map about its mean indicates that the tails of the distribution are nearly Gaussian. Further work was done to investigate whether this was a simple happenstance or if there were other parameter values for which the deterministic fluctuations about the mean value of the y map were Gaussian. Table 1 lists several values of the parameters μ_X , μ_Y , and for which Gaussian fluctuations about the mean of the long-term behavior of the y map were obtained.

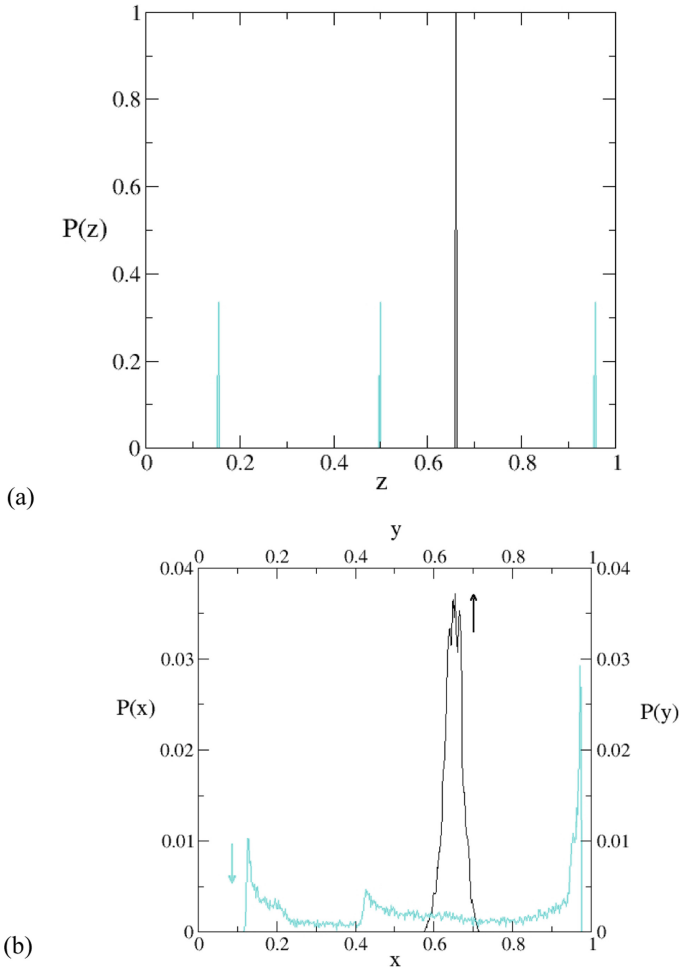


Fig. 4. The behavior (represented as a pdf) of the (a) uncoupled and (b) coupled x_n (blue/grey) and y_n (black) maps at their values of $\mu_X = 3.832$ and $\mu_Y = 2.95$ respectively, for an $\varepsilon = 0.050$.

The effect of the mixing trajectories for one set of parameters is demonstrated in Fig. 4. Part (a) of Fig. 4 shows the long term behavior of the uncoupled ($\varepsilon = 0$) x and y maps for $\mu_X = 3.832$ and $\mu_Y = 2.95$ by plotting the long term behavior of the z map at values of $\mu = \mu_X$ and $\mu = \mu_Y$, respectively, as a probability distribution function (pdf). Once the uncoupled y map (z for $\mu = 2.95$) reaches its equilibrium value (dark/black line), there is a 100% chance of finding it at the fixed point. Likewise, the uncoupled x map (z for $\mu = 3.832$) has reached its period-3 orbit after a few iterations and so there is a 1/3 probability of finding it at any of the three locations (light/blue lines) in its long term behavior when the maps are uncoupled ($\varepsilon = 0$). Part (b) of Fig. 4 demonstrates the pdf behavior in terms of $P(x)$ and $P(y)$ when $\varepsilon = 0.050$. The consequence of mixing for the x map is to effectively push μ_X higher and into the nearby chaotic behavior. While

Table 1. Values of μ_X , μ_Y , and ε

Set	μ_X	μ_Y	ε
<u>1</u>	3.840	3.00	0.025
<u>2</u>	3.830	3.00	0.050
<u>3</u>	3.808	3.00	0.075
<u>4</u>	3.810	2.95	0.025
<u>5</u>	3.832	2.95	0.050
<u>6</u>	3.826	2.90	0.025

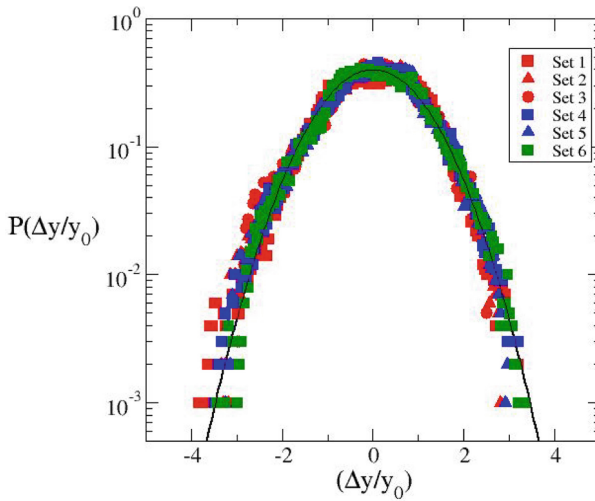


Fig. 5. The normalized values of the long-term behavior of the coupled y_n map relative to the mean as a pdf. The fluctuations from the deterministic map form a nearly Gaussian distribution (solid black line). The symbol legend conforms to the data in Table 1.

the coupling maintains the stability of the y map and pushes the fixed point slightly lower (the mean of $y \sim 0.649$ for $P(y)$ in Fig. 4(b) is slightly smaller than the fixed point of $y = 0.66$ in Fig. 4(a)), the coupling introduces fluctuations about the mean even in the long term behavior of the map.

The flatness of these fluctuations about the mean value for $P(y)$ is $F = 3$ as shown by the box in the plot of Fig. 3, indicating the fluctuations in the tails are nearly Gaussian. While there are examples of large fluctuations elsewhere in the graph, it should be noted that the box highlights an occurrence where the flatness is gently changing and is not discontinuous. To observe this Gaussian more clearly, Fig. 5 is a log plot of $P(\Delta y / y_0)$ where $\Delta y = y - y_{\text{mean}}$ and y_0 is the variance of the fluctuations about the mean value. A Gaussian curve is shown for comparison. The fluctuations for all values of μ_X , μ_Y , and ε as listed in Table 1 are plotted. Each histogram in the plot is composed of 20,000

iterations of the coupled y map. A general trend was that for larger values of μ_Y the larger the window in ϵ that could produce an occurrence of Gaussian statistics for some value of μ_X .

3 Conclusions

We have reported on the results of a pair of coupled logistic maps that produce Gaussian fluctuations about the mean of the stable map due to the unstable map's chaotic behavior. The results give an example of a pair of deterministic equations that together produce a set of equilibrium-like fluctuations in one of the two maps and are applicable to the chaotic encryption of data to hide information within an apparently random, but deterministically generated signal. It is an interesting question for further study if this map is an example of a broader class of coupled maps that will demonstrate this general behavior. Additionally, the results demonstrate a new low dimensional example of a system for which equilibrium thermostatics can be recaptured in a system driven out of equilibrium, rather than a more complicated system of higher dimensionality. In the former, the apparently random fluctuations produced from a deterministic set of equations can be used to encrypt a signal or an image for security purposes, with multiple sets of different parameters that all demonstrate noise-like Gaussian fluctuations from deterministic equations. In the latter, the mixing improves the stability of one trajectory while increasing the instability of the other and may shed new light on the non-equilibrium behavior of low-dimensional experiments such as a dimer on a shaken plate. In subsequent papers, we will demonstrate a simple technique for using these coupled logistic maps at these parameters for the purposes of image encryption, similar to recent work, as well as an application to the low-dimensional granular system to build a simple picture of non-equilibrium thermodynamics. Such cross-disciplinary results are one of the hallmarks and strengths of research in nonlinear dynamics.

The authors acknowledge the support in part by funds from the Vice Provost for Research and the NSF REU Program at Baylor University.

References

1. Feigenbaum, M.J.: Quantitative universality for a class of nonlinear transformations. *J. Stat. Phys.* **19**, 25 (1978)
2. Egolf, D.A.: Equilibrium regained: From nonequilibrium chaos to statistical mechanics. *Science* **287**, 101 (2000)
3. Baxter, G.W., Olafsen, J.S.: Experimental evidence for molecular chaos in granular gases. *Phys. Rev. Lett.* **99** 028001 (2007)
4. Borges, E.P., Tsallis, C., Ananos, G.F.J., de Oliveira, P.M.C.: Nonequilibrium probabilistic dynamics of the logistic map at the edge of chaos. *Phys. Rev. Lett.* **89**, 254103 (2002)
5. Pisarchik, A.N., Flores-Carmona, N.J., Carpio-Valadez, M.: Encryption and decryption of images with chaotic map lattices. *Chaos* **16**, 033118 (2006)
6. Phatak, S.C., Sburesh Rao, S: Logistic map: a possible random number generator. *Phys. Rev. E*, **51**, 3670 (1995)
7. Dorbolo, S., Volfson, D., Tsimring, L., Kudrolli, A.: Dynamics of a bouncing dimer. *Phys. Rev. Lett.* **95**, 044101 (2005)

8. Luck, J.M., Mehta, A.: Bouncing ball with a finite restitution: Chattering, locking and chaos. *Phys. Rev. E* **48**, 3988 (1993)
9. Elhadj, Z., Sprott, J.C.: The effect of modulating a parameter in the logistic map. *Chaos* **18**, 023119 (2008)
10. Pastor-Diaz, I., Lopez-Fraguas, A.: Dynamics of two coupled van der Pol oscillators. *Phys. Rev. E* **52**, 1480 (1995)
11. Atwell, J., Olafsen, J.S.: Anisotropic dynamics in a shaken granular dimer gas experiment. *Phys. Rev. E* **71**, 062301 (2005)
12. Oteo, J.A., Ros, J.: Double precision errors in the logistic map: Statistical study and dynamical interpretation. *Phys. Rev. E* **76**, 036214 (2007)
13. McQuarrie, D.A.: *Mathematical Methods for Scientists and Engineers*. University Science Books, Sausalito, California (2003)
14. Weiss, J.B.: Moments of the probability distribution for noisy maps. *Phys. Rev. A* **35**, 879 (1987)
15. Hu, Dong, Y.: Quantum color image encryption based on a novel 3D chaotic system. *J. Appl. Phys.* **131**, 114402 (2022)